Electron-impact excitation of $n = 2$ levels of helium at intermediate energies

K. Bhadra, J. Callaway, and Ronald J. W. Henry
Louisiana State University, Baton Rouge, Louisiana 70803
(Received 27 November 1978)

Five-state close-coupling equations for electron-helium scattering are solved in the energy region from 30 to 100 eV. Integral and differential cross sections for excitation of the ground state to the $n = 2$ states 2^3S, 2^1S, 2^3P^0, and 2^1P^0 are presented. Calculated shapes of differential cross sections versus angle for various energies are in fair agreement with measurements, but the magnitudes of the cross sections are overestimated. Allowance for coupling between 2^3S and 2^3P^0 brings calculated differential cross sections into good quantitative agreement with experiment.

I. INTRODUCTION

A five-state close-coupling approximation has been applied to the scattering of electrons and the excitation of the $n=2$ states of atomic helium for a range of incident energies between 29.6 and 100 eV. This range has been studied theoretically in various approximations, and both calculations and measurements have been reviewed recently by Bransden and McDowell.[1] No theoretical methods have produced results in this energy range which give good agreement simultaneously with the experimental shape of the cross section versus energy and differential cross section versus angle for excitation to 2^3S, 2^1S, 2^3P^0, and 2^1P^0.

Theoretical methods which have been used in this intermediate energy range to calculate differential cross sections for excitation to some of the $n=2$ states include a first Born approximation and Born augmented by various first-order exchange amplitudes.[2] These approximations predict correct angle dependence for small momentum transfers but are orders of magnitude too small at large momentum transfers. Similar failings are evident for calculations in a Vainstein approximation,[3] Glauber,[4] and multichannel eikonal approximation.[5] Joachain and Vanderpoorten[6] use an eikonal distorted-wave method but limit their discussion to small-angle scattering. A second-order potential method[7] which employs an impact-parameter formalism is not expected to be accurate for impact energies below 300 eV.

A distorted-wave (DW) approach has been applied with success in the intermediate energy range in a calculation of excitation of the 2^1P^0 state by Madison and Shelton.[8] In this work, both the incident and scattered waves are assumed to be distorted by the static potential produced by the He atom in its ground state. Hidalgo and Geltman[9] used a Coulomb-projected Born (CPB) approximation which, although it neglects exchange, does allow for an interaction between the incident electron and the nucleus. They obtained differential cross sections for 2^1S and 2^1P^0 excitation which are much greater than those given by the ordinary Born approximation at large scattering angles. A second-order potential method (SOPDW) in which a partial-wave formalism is used, has been applied with success by Bransden and Winters[10] to excitation of the 2^1S and 2^3S states. Finally, two methods have been used in the intermediate energy region to calculate cross sections for excitation to the four $n=2$ states. There are various distorted-wave polarized-orbital methods[11,12] (DWPO) and a first-order many-body theory (MBT).[13]

Scott and McDowell[11] found that the DWPO method reproduces well the shape of the differential cross section for excitation of 2^1S, but that the depth of the minima were not accurately predicted. In addition, the DWPO model is considerably less successful in predicting differential cross sections of the 2^3S state. For excitation of 2^1P^0, Scott and McDowell's DWPO model[12] gave good agreement with experiment for energies 29.6 and 40.1 eV at angles $\theta < 60°$, but a differential cross section was predicted which is much too low at larger angles. Again, for excitation of the triplet state 2^3P^0, the DWPO model was considerably less successful than in the case of 2^1P^0.

Thomas *et al.*[13] used a first-order method based on many-body theory to obtain excellent results for excitation of 2^1P^0 for energies over 40 eV in the whole angular range except for angles less than 15°. For excitation of 2^1S, the main feature of a strong minimum around 50° is predicted. However, similarly to the DWPO model, the MBT procedure was considerably less accurate in predicting angular distributions for excitation of 2^3S and 2^3P^0.

The two major factors limiting the accuracy achieved by a close-coupling approximation are the number of states included in the expansion and

the choice of atomic states to be used.

We have included in the close-coupling expansion only the five atomic states involved in the excitation process, 1^1S, 2^3S, 2^1S, 2^3P^0, and 2^1P^0. We anticipate that convergence of the expansion with respect to inclusion of various pseudostates will be the subject of a further study. At present we attempt to obtain the correct qualitative behavior of the differential cross sections for the various excitation processes. Neglect of the higher states is expected to cause an overestimate of the calculated excitation cross sections.[14] Addition of pseudostates may decrease excitation cross sections as occurs, for example, with H,[15] He^+,[16] and Be^+.[17]

The atomic eigenstates used in our calculations are constructed from three Slater-type orbitals which we label $1s$, $2s$, and $2p$. The $1s$ orbital is the three-parameter ground-state orbital given by Clementi.[18] The $2s$ orbital is obtained with the CIV3 program of Hibbert[19] and is optimized simultaneously on the energies of the 2^3S and 2^1S excited states. We obtain

$$P_{2s}(r) = 0.964\,15 r\, e^{-0.86r} - 0.677\,49 r^2 e^{-0.65r} + 0.152\,52 r^3 e^{-0.9843r}.$$

Similarly, the $2p$ orbital is optimized on the energies of the 2^3P^0 and 2^1P^0 excited states, and is given by

$$P_{2p}(r) = 0.225\,23 r^2 e^{-0.520\,07r}.$$

The configuration-interaction functions for the target states are represented by

$$1^1S, 2^1S: \; c_1 1s^2 + c_2 1s2s + c_3 2s^2 + c_4 2p^2,$$

$$2^3S: \; 1s2s,$$

$$2^3P^\circ, 2^1P^\circ: \; c_1 1s2p + c_2 2s2p.$$

Table I gives the c_i coefficients together with the corresponding eigenenergies relative to the 1^1S level. The final two columns give the energy differences calculated by Berrington *et al.*,[20] who used a more elaborate configuration-interaction wave function in their study of excitation of the $n=2$ states at energies below 25 eV, and the experimental energy differences from the tables of Moore.[21] Calculated energy differences are in fair agreement with experiment and with the results of Berrington *et al.* However, the oscillator strength for our wave functions for 1^1S-2^1P^0 is 0.341 and 0.318 in the dipole length and dipole velocity approximations, respectively. This compares with 0.279 obtained in both length and velocity approximations in more elaborate structure calculations.[22]

Since cross sections at large values of angular momentum L are directly proportional to the oscillator strength calculated in the dipole length approximation, we anticipate that in a high-energy limit where the Bethe approximation is valid, we would overestimate the optical excitation cross section by 22%. In addition, at lower energies we anticipate that use of a truncated (nonconverging) close-coupling expansion will lead to overestimation of the excitation cross sections. Thus the magnitude of our cross sections will be too large, but the relative shape of the differential cross section may be reasonable.

Comparison of our results will be made in Sec. II with DWPO, MBT, DW, CPB, and SOPDW theories as well as with experimental results.

II. RESULTS

The integro-differential equations which arise in the close-coupling approximation are solved by means of a noniterative integral equation method (NIEM).[23] The basic step size at small values of the radial distance r is $0.01a_0$. Exchange terms are neglected at $r = 22.3a_0$, where the longest-ranged orbital has fallen to less than 10^{-3}.

A check on the accuracy and CPU times of the NIEM program was made with an R-matrix computer program.[24] This was made at a preliminary stage of the calculation, when the best orbitals had not been determined. Thus the partial cross sections quoted in Table III differ from those which contribute to the integral cross sections given in Table IV. For the R-matrix program it was necessary to use 25 continuum orbitals for each scat-

TABLE I. Coefficients of configurations in atomic states.

State	c_1	c_2	c_3	c_4	Energy (a.u.)	a	b
1^1S	−0.9993	0.005 06	0.009 33	0.005 51	0.0	0.0	0.0
2^3S	1.0				0.7397	0.7105	0.7284
2^1S	0.006 60	0.994 51	0.103 83	0.010 68	0.7639	0.7397	0.7577
2^3P^o	0.997 58	0.069 58			0.7751	0.7511	0.7705
2^1P^o	0.996 84	0.079 45			0.7879	0.7605	0.7798

[a] Berrington *et al.* (Ref. 20).
[b] Moore (Ref. 21).

TABLE II. CPU time (SEC) for R matrix and NIEM programs.

	NIEM		R matrix		
L	POTCC	NIE	STG1	STG2	STG3
0	9	344	1105	9	191
1	16	1063		18	751
2	9	497		17	539
3	6	317		16	536

tering function, and exchange terms are neglected at $r=19a_0$, where the longest-ranged orbital had fallen to less than 10^{-2}. A grid of 600 mesh points was used.

Representative times for the various stages of each computer program for an IBM 3033 are given in Table II. For the R-matrix program, in STG1 the continuum orbitals are set up for $L=0$–8 and so this is run once for the first nine L values. In STG2, the time is independent of the number of energy values, and STG3 times are quoted for five energies. For the NIEM program, the POTCC times are independent of the number of energy values and the NIEM times are for five energies. Different times occur for $L=0$, 1, 2, and 3, since there are a different number of bound states in each case. Times are the same for higher L as for $L=3$. The R-matrix program is faster for $L=0$ and 1 but there is considerable overhead in setting up STG1. For higher L values, the NIEM program is faster, independent of the number of energies to be evaluated.

Results from the alternative methods of solving the integro-differential equations are in satisfactory agreement. Representative partial cross sections at two energies for $L=0$ and 3 are given in Table III.

Partial cross sections for forbidden transitions fall off rapidly with increasing L and truncation of the partial wave sum at $L=12$ is sufficient to achieve a cross-section sum accurate to 1% at the highest energy considered. For the optically allowed 1^1S-2^1P^0 cross section, values of L up to 47 are retained to make the cross-section sum converge to within 1%. For $L \geq 13$, the nonexchange close-coupling equations are solved by means of the NIEM. For $L \geq 25$, a unitarized Born approximation is used. The differential cross sections are obtained from the reactance matrices calculated by the NIEM program, with a computer program of Brandt *et al.*[25]

TABLE III. Partial cross sections ($1^1S-n^{2S+1}L$) obtained with NIEM program (N) and R matrix program (R).

	$L=0$			
$n^{2S+1}L$	2.175 Ry		7.35 Ry	
L	R	N	R	N
1^1S	1.6998	1.6989	0.3825	0.3836
2^3S	0.02339	0.02363	0.00077	0.00082
2^1S	0.02302	0.02326	0.00700	0.00732
2^3P^o	0.00828	0.00836	0.00029	0.00030
2^1P^o	0.01302	0.01314	0.00427	0.00429
	$L=3$			
1^1S	0.01092	0.01051	0.00612	0.00625
2^3S	0.00327	0.00327	0.00006	0.00006
2^1S	0.00438	0.00444	0.01801	0.01816
2^3P^o	0.00525	0.00525	0.00041	0.00041
2^1P^o	0.08396	0.08404	0.01970	0.01979

Integral cross sections at scattering energies of 29.6, 40.1, 60, 80, and 100 eV for elastic scattering and for excitation to the 2^3S, 2^1S, 2^3P^0, and 2^1P^0 are given in Table IV. As explained in the Introduction, the excitation cross section values are higher than experimental values.

Results for differential cross sections are given in Tables VI–IX and Figs. 1–17.

A. Differential elastic cross sections for helium

There are as yet no published measurements in the energy range considered here except at 100 eV. For the energy range 100–500 eV, Jansen *et al.*[26] have surveyed the present status of experiments. Figure 1 compares our results for 100 eV in a five-state close-coupling approximation with the results of Jansen *et al.* for the angular range $5 \leq \theta \leq 50°$, and with those of Kurepa and Vuskovic[27] for $50 \leq \theta \leq 150°$. Following Bransden and McDow-

TABLE IV. Integral cross sections[a] in units of πa_0^2 in 5CCX.

E (eV)	29.6	40.1	60	80	100
Transition					
1^1S-1^1S	2.251	1.690	1.118	0.816	0.635
1^1S-2^3S	0.573 −1	0.177 −1	0.494 −2	0.224 −2	0.125 −2
1^1S-2^1S	0.958 −1	0.656 −1	0.460 −1	0.362 −1	0.302 −1
1^1S-2^3P^o	0.895 −1	0.440 −1	0.122 −1	0.452 −2	0.209 −2
1^1S-2^1P^o	0.122	0.169	0.183	0.176	0.163

[a] The negative number in each entry is an exponent of 10 by which the cross-section value should be multiplied.

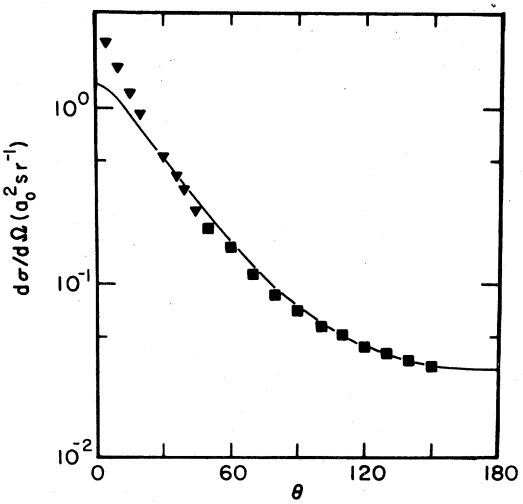

FIG. 1. Differential elastic cross section at incident electron energy of 100 eV. Symbols are given in Table V.

ell,[1] we normalize Kurepa and Vuskovic's data to the results of Jansen *et al.* at 50°. Present calculations are in very good agreement with experiment except at small angles, where omission of 100% polarizability of the target leads to smaller forward elastic cross sections. Table VI summarizes our calculations at five electron-scattering energies.

B. 1^1S-$2\,^1P^o$ excitation of helium

Table VII and Figs. 2–5 give the present results in a five-state close-coupling approximation. In Figs. 2 and 3, at 29.6 and 40.1 eV, the experimental results of Truhlar *et al.*[28] are compared with MBT calculations of Thomas *et al.*,[13] DWPO calculations of Scott and McDowell,[11] DW calculations of Madison and Shelton,[8] and the present calculations. Figure 4, for 80 eV, compares theoretical cross sections of Thomas *et al.*,[13] Hidalgo and Geltman,[9] and the present results with measurements of Chutjian and Srivastava,[29] Truhlar *et al.*,[28] and Opal and Beaty.[30] In Fig. 5, for 100 eV, the experimental data are those of Suzuki and

TABLE V. Symbols used to represent various approximations or measurements in the figures.

———	Present 5CCX calculations.
— — —	Hidalgo and Geltman (Ref. 9)
·····	Madison and Shelton (Ref. 8)
— — — —	Thomas *et al.* (Ref. 13)
— · · —	Scott and McDowell (Refs. 11, 12).
□	Trajmar (Ref. 32).
○	Hall *et al.* (Ref. 33).
▲	Truhlar *et al.* (Ref. 28).
+	Chutjian and Srivastava (Ref. 29).
◇	Opal and Beaty (Ref. 30).
▽	Suzuki and Takayanagi (Ref. 31).
●	Rice *et al.* (Ref. 34).
×	Vriens *et al.* (Ref. 35).
△	Yagashita *et al.* (Ref. 36).
▼	Jansen *et al.* (Ref. 26).
■	Kurepa and Vuskovic (Ref. 27).

TABLE VI. Differential elastic cross sections[a] in units of a_0^2 sr^{-1}.

θ \ E (eV)	29.6	40.1	60	80	100
0	1.83	1.73	1.63	1.42	1.31
10	1.67	1.54	1.32	1.13	1.01
20	1.42	1.24	1.01	0.84	0.74
30	1.17	0.98	0.76	0.62	0.53
40	0.95	0.77	0.57	0.45	0.37
50	0.76	0.60	0.43	0.32	0.25
60	0.62	0.48	0.33	0.24	0.18
70	0.51	0.39	0.26	0.18	0.13
80	0.44	0.33	0.21	0.14	0.96 −1
90	0.40	0.29	0.17	0.11	0.74 −1
100	0.38	0.27	0.15	0.90 −1	0.60 −1
110	0.37	0.25	0.13	0.78 −1	0.51 −1
120	0.37	0.24	0.12	0.69 −1	0.44 −1
130	0.38	0.23	0.11	0.63 −1	0.39 −1
140	0.39	0.23	0.11	0.58 −1	0.36 −1
150	0.40	0.23	0.10	0.56 −1	0.34 −1
160	0.41	0.23	0.10	0.54 −1	0.33 −1
170	0.42	0.23	0.10	0.53 −1	0.32 −1
180	0.42	0.24	0.10	0.54 −1	0.33 −1

[a]The negative number in each entry is the exponent of 10 by which the cross-section value should be multiplied.

TABLE VII. Differential cross sections[a] for $1\,^1S$-$2\,^3S$ in units of a_0^2 sr^{-1}.

θ \ E (eV)	29.6	40.1	60	80	100
0	0.40 −1	0.30 −1	0.13 −1	0.71 −2	0.42 −2
10	0.37 −1	0.27 −1	0.11 −1	0.63 −2	0.29 −2
20	0.30 −1	0.19 −1	0.57 −2	0.22 −2	0.10 −2
30	0.21 −1	0.10 −1	0.18 −2	0.58 −2	0.41 −3
40	0.13 −1	0.43 −2	0.22 −3	0.31 −3	0.38 −3
50	0.92 −2	0.19 −2	0.47 −4	0.30 −3	0.30 −3
60	0.10 −1	0.16 −2	0.11 −3	0.22 −3	0.20 −3
70	0.14 −1	0.17 −2	0.86 −4	0.15 −3	0.14 −3
80	0.18 −1	0.14 −2	0.63 −4	0.15 −3	0.12 −3
90	0.18 −1	0.84 −3	0.15 −3	0.21 −3	0.15 −3
100	0.15 −1	0.47 −3	0.40 −3	0.31 −3	0.18 −3
110	0.97 −2	0.84 −3	0.81 −3	0.45 −3	0.23 −3
120	0.52 −2	0.22 −2	0.13 −2	0.58 −3	0.27 −3
130	0.45 −2	0.46 −2	0.19 −2	0.70 −3	0.30 −3
140	0.92 −2	0.76 −2	0.25 −2	0.81 −3	0.33 −3
150	0.19 −1	0.11 −1	0.30 −2	0.90 −3	0.35 −3
160	0.30 −1	0.14 −1	0.34 −2	0.95 −3	0.36 −3
170	0.39 −1	0.17 −1	0.37 −2	0.10 −2	0.37 −3
180	0.42 −1	0.16 −1	0.37 −2	0.10 −2	0.38 −3

[a]The negative number in each entry is the exponent of 10 by which the cross-section value should be multiplied.

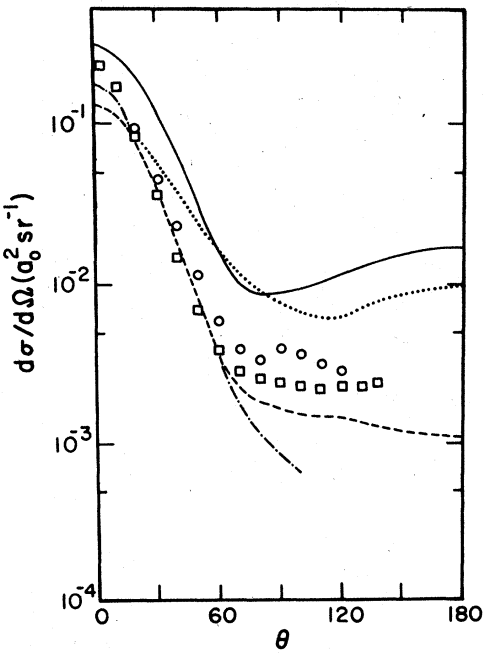

FIG. 2. Differential cross section for 1^1S-2^1P^0 at incident electron energy of 29.6 eV. Symbols are given in Table V.

Takayanagi,[31] and the theory that of Scott and McDowell,[11] Hidalgo and Geltman,[9] and the present calculations. While the present results are in reasonably good agreement with the shape of the

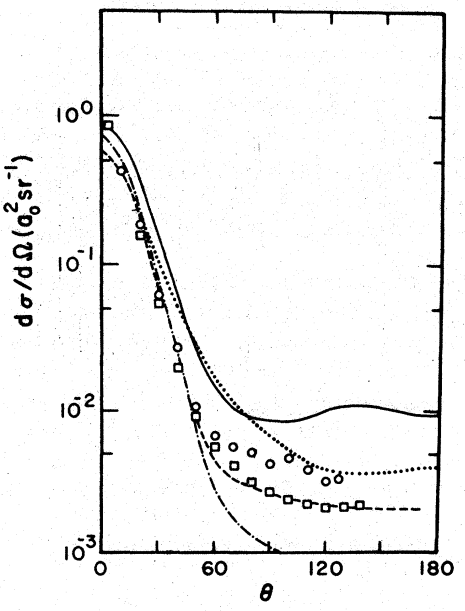

FIG. 3. Differential cross section for 1^1S-2^1P^0 at incident electron energy of 40.1 eV. Symbols are given in Table V.

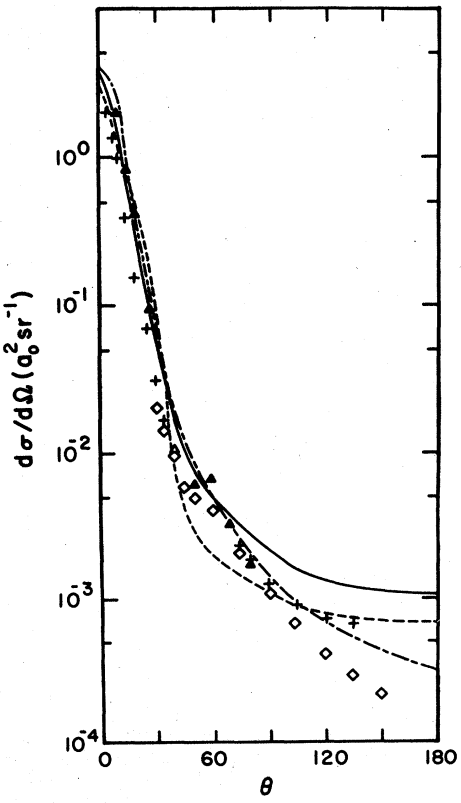

FIG. 4. Differential cross section for 1^1S-2^1P^0 at incident electron energy of 80 eV. Symbols are given in Table V.

differential cross section, the MBT method clearly gives superior cross sections, particularly at lower energies. The 2^1P^0 differential cross section is dominated by forward scattering, which is overestimated in the present calculation as is the minor backward angle component. Flux loss to other channels not included in the present close-coupling calculation is probably the dominant cause of the overestimation of the cross section. Integral cross sections for excitation of 2^1P^0 are approximately 50% higher than experimental cross sections at 100-eV scattering energy.

C. 1^1S-$2\,^1S$ excitation of helium

Table VIII and Figs. 6–9 give results of the present five-state close-coupling approximation (5 CCX) calculation. In Figs. 6 and 7 for 29.6 and 40.1 eV we compare 5 CCX, DWPO, and MBT theories with the measurements of Trajmar[32] and Hall *et al.*[33] The deep minimum near 50° is well reproduced in the present calculations, but the cross section is greatly overestimated at backward scattering angles. Figure 8 compares the

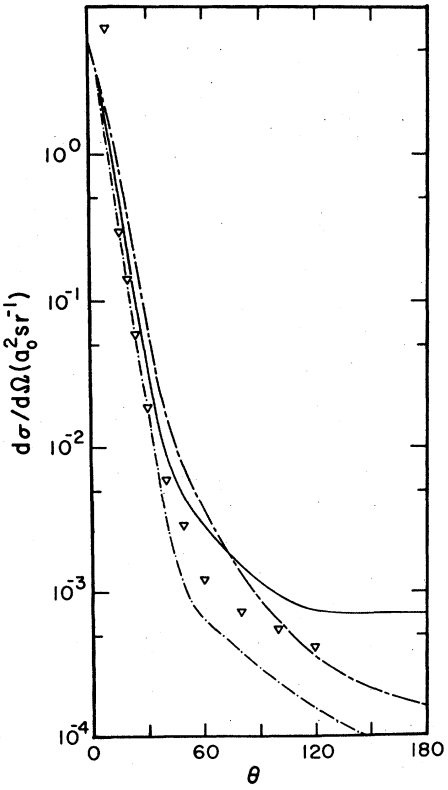

FIG. 5. Differential cross section for $1^1S-2^1P^0$ at incident electron energy of 100 eV. Symbols are given in Table V.

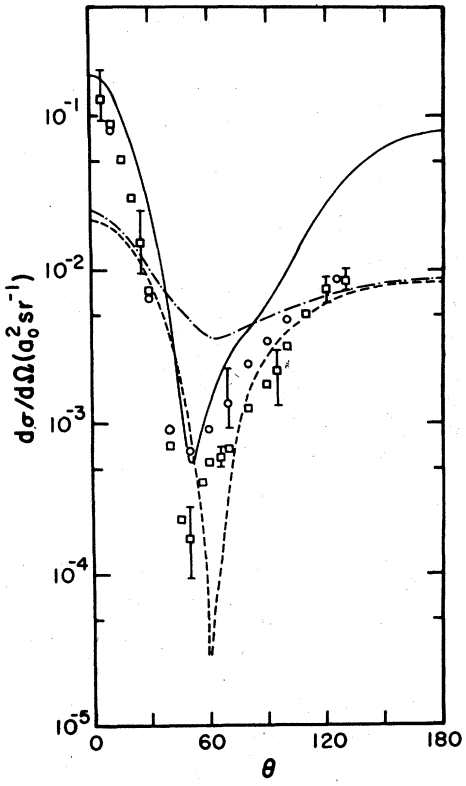

FIG. 6. Differential cross section for 1^1S-2^1S at incident electron energy of 29.6 eV. Symbols are given in Table V.

TABLE VIII. Differential cross sections[a] for 1^1S-2^1S in units of a_0^2 sr^{-1}.

E (eV) θ	29.6	40.1	60	80	100
0	0.18	0.28	0.44	0.53	0.58
10	0.14	0.18	0.19	0.16	0.14
20	0.77 −1	0.55 −1	0.41 −1	0.39 −1	0.39 −1
30	0.26 −1	0.11 −1	0.13 −1	0.14 −1	0.13 −1
40	0.50 −2	0.22 −2	0.45 −2	0.54 −2	0.54 −2
50	0.60 −3	0.40 −3	0.25 −2	0.40 −2	0.41 −2
60	0.13 −2	0.68 −4	0.34 −2	0.45 −2	0.41 −2
70	0.27 −2	0.10 −2	0.51 −2	0.50 −2	0.39 −2
80	0.41 −2	0.30 −2	0.64 −2	0.50 −2	0.35 −2
90	0.64 −2	0.57 −2	0.72 −2	0.48 −2	0.31 −2
100	0.11 −1	0.91 −2	0.77 −2	0.45 −2	0.27 −2
110	0.81 −1	0.13 −1	0.81 −2	0.42 −2	0.24 −2
120	0.27 −1	0.18 −1	0.84 −2	0.40 −2	0.22 −2
130	0.39 −1	0.24 −1	0.88 −2	0.39 −2	0.20 −2
140	0.52 −1	0.30 −1	0.92 −2	0.38 −2	0.19 −2
150	0.63 −1	0.36 −1	0.96 −2	0.38 −2	0.18 −2
160	0.73 −1	0.41 −1	0.10 −1	0.38 −2	0.17 −2
170	0.79 −1	0.45 −1	0.10 −1	0.38 −2	0.17 −2
180	0.81 −1	0.46 −1	0.10 −1	0.37 −2	0.17 −2

[a] The negative number in each entry is the exponent of 10 by which the cross-section value should be multiplied.

three calculations and those of the Hidalgo and Geltman[9] and Bransden and Winters[10] with the measurements of Opal and Beaty[30] and Rice *et al.*[34] at 80 eV, and in Fig. 9, the present results and calculations in CPB and SOPDW approximations are compared with the experimental determinations of Vriens *et al.*[35] and Suzuki and Takayanagi[31] at 100 eV. The magnitude of the backward-scattering component falls rapidly with increasing energy for energies above 50 eV, and consequently the dip around 50° in the differential cross section becomes more shallow. Thus forward scattering dominates for energies above 50 eV and the 5 CCX results become closer in magnitude to experimental values as the energy increases. However, although the present results agree well with the shape of the differential cross section, the integral cross section is still a factor of 2 larger than that given by experiment at 100 eV.

D. $1^1S-2^3P^0$ excitation of helium

Table IX and Figs. 10–13 give results of the present calculation. These are compared with the

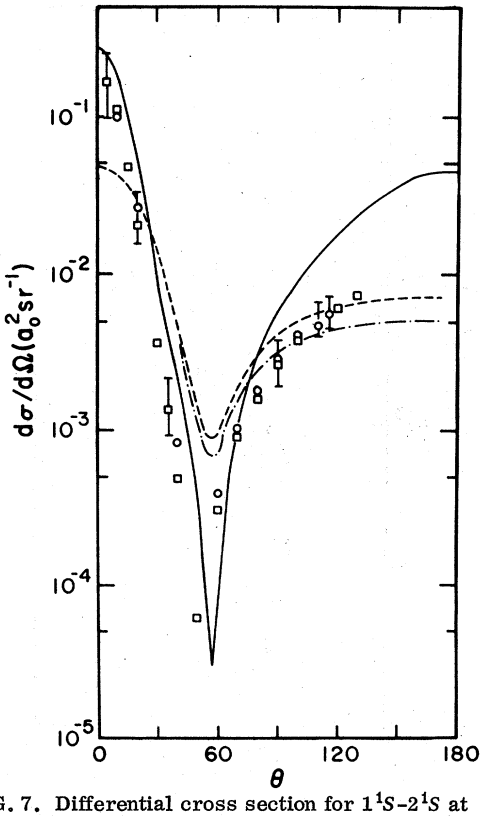

FIG. 7. Differential cross section for 1^1S-2^1S at incident electron energy of 40.1 eV. Symbols are given in Table V.

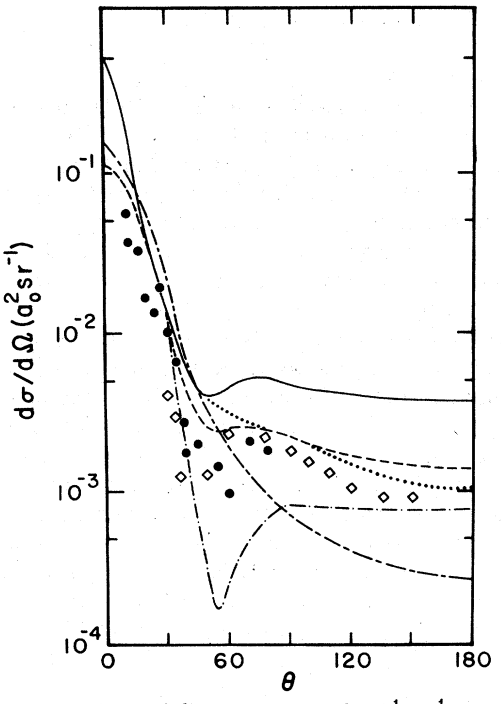

FIG. 8. Differential cross section for 1^1S-2^1S at incident electron energy of 80 eV. Symbols are given in Table V.

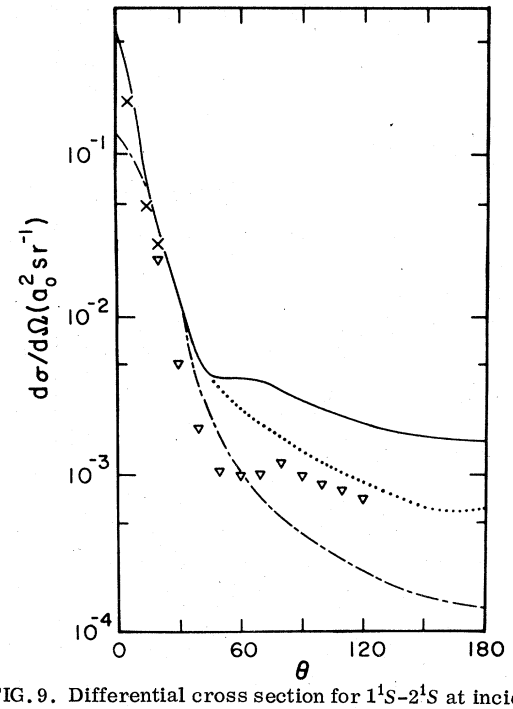

FIG. 9. Differential cross section for 1^1S-2^1S at incident electron energy of 100 eV. Symbols are given in Table V.

cross section measurements of Trajmar[32] and Hall *et al.*[33] and with the theoretical cross sections of Thomas *et al.*[13] in Figs. 10 and 11 for 29.6 and 40.1 eV. Figure 12 compares theory with the measurements of Opal and Beaty,[30] Yaga-

TABLE IX. Differential cross sections [a] for $1\ ^1S$-$2\ ^3P^0$ in units of a_0^2 sr^{-1}.

θ \ E (eV)	29.6	40.1	60	80	100
0	0.20 −1	0.20 −1	0.88 −2	0.42 −2	0.23 −2
10	0.20 −1	0.22 −1	0.10 −1	0.56 −2	0.34 −2
20	0.21 −1	0.25 −1	0.13 −1	0.71 −2	0.43 −2
30	0.23 −1	0.27 −1	0.13 −1	0.61 −2	0.31 −2
40	0.25 −1	0.25 −1	0.10 −1	0.37 −2	0.16 −2
50	0.25 −1	0.21 −1	0.62 −2	0.19 −2	0.66 −3
60	0.22 −1	0.15 −1	0.35 −2	0.91 −3	0.30 −3
70	0.19 −1	0.10 −1	0.20 −2	0.50 −3	0.16 −3
80	0.17 −1	0.75 −2	0.14 −2	0.33 −3	0.11 −3
90	0.17 −1	0.65 −2	0.11 −2	0.27 −3	0.84 −4
100	0.21 −1	0.67 −2	0.10 −2	0.23 −3	0.70 −4
110	0.26 −1	0.73 −2	0.72 −3	0.19 −3	0.60 −4
120	0.30 −1	0.75 −2	0.80 −3	0.16 −3	0.48 −4
130	0.32 −1	0.70 −2	0.65 −3	0.12 −3	0.39 −4
140	0.28 −1	0.58 −2	0.48 −3	0.95 −4	0.33 −4
150	0.21 −1	0.41 −2	0.32 −3	0.69 −4	0.26 −4
160	0.12 −1	0.24 −2	0.18 −3	0.51 −4	0.22 −4
170	0.52 −2	0.11 −2	0.91 −4	0.41 −4	0.21 −4
180	0.25 −2	0.62 −3	0.57 −4	0.36 −4	0.20 −4

[a] The negative number in each entry is the exponent of 10 by which the cross section is to be multiplied.

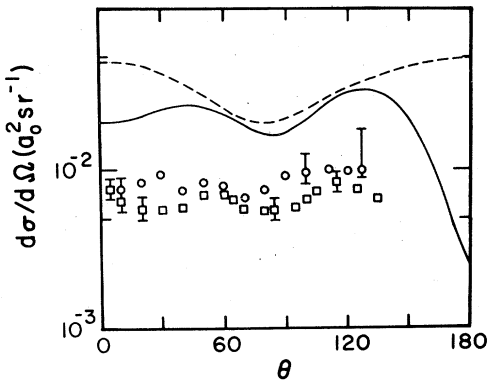

FIG. 10. Differential cross section for 1^1S-$2\,^3P^0$ at incident electron energy of 29.6 eV. Symbols are given in Table V.

shita *et al.*,[36] and Chutjian and Srivastava.[29] Present results favor the experimental cross sections of Chutjian and Srivastava and Yagashita *et al.* for scattering angles less than 40°. Measurements of Suzuki and Takayanagi[31] and Yagashita *et al.* are compared with the five-state close-coupling calculations in Fig. 13. The shape of the differential cross section in the present calculations is in very good accord with that found experimentally at the four energies considered. The differential cross section has two shallow peaks at energies less than 50 eV, and the first peak moves to lower angles as the energy is increased. For energies above 50 eV, the peak occurs at

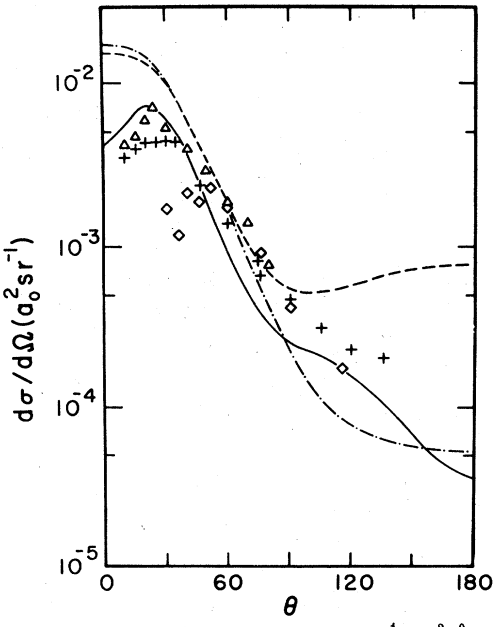

FIG. 12. Differential cross section for 1^1S-$2\,^3P^0$ at incident electron energy of 80 eV. Symbols are given in Table V.

20°. The 5 CCX approximation predicts a sharp decrease of the cross section at large backward scattering angles (>140°), in contrast to that predicted in the MBT approximation. A major difference between 5 CCX and MBT is that in the present calculation the $2\,^3S$ and $2\,^3P^0$ states are coupled together. Allowance for this coupling,

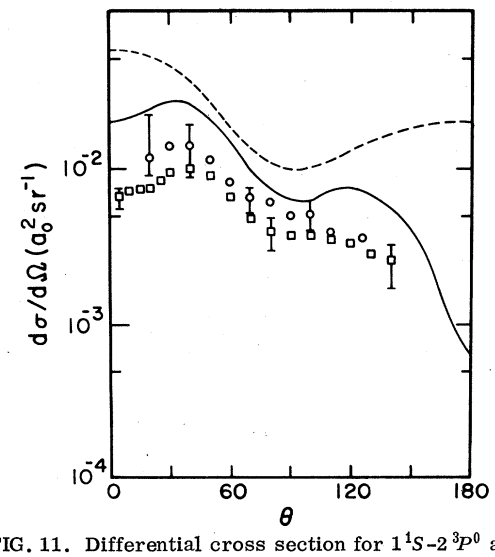

FIG. 11. Differential cross section for 1^1S-$2\,^3P^0$ at incident electron energy of 40.1 eV. Symbols are given in Table V.

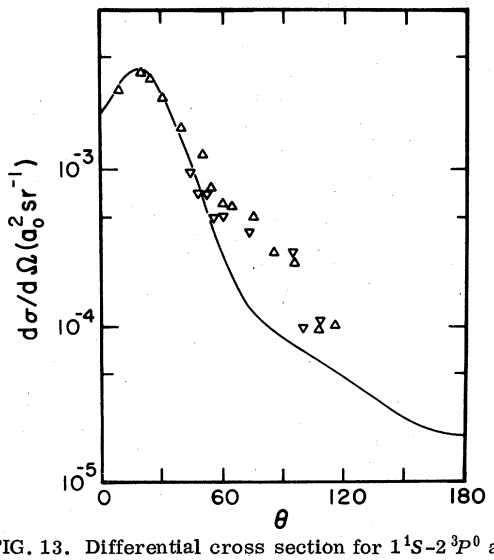

FIG. 13. Differential cross section for 1^1S-$2\,^3P^0$ at incident electron energy of 100 eV. Symbols are given in Table V.

TABLE X. Differential cross sections[a] for $1\,^1S$-$2\,^1P^0$ in units of a_0^2 sr^{-1}.

E (eV) / θ	29.6	40.1	60	80	100
0	0.30	0.84	2.26	3.90	5.55
10	0.27	0.67	1.26	1.49	1.67
20	0.20	0.36	0.41	0.32	0.24
30	0.12	0.16	0.11	0.65 −1	0.37 −1
40	0.62 −1	0.62 −1	0.32 −1	0.16 −1	0.88 −2
50	0.31 −1	0.26 −1	0.14 −1	0.75 −2	0.44 −2
60	0.16 −1	0.15 −1	0.92 −2	0.51 −2	0.30 −2
70	0.10 −1	0.11 −1	0.71 −2	0.37 −2	0.21 −2
80	0.88 −2	0.95 −2	0.55 −2	0.27 −2	0.15 −2
90	0.88 −2	0.87 −2	0.44 −2	0.21 −2	0.12 −2
100	0.95 −2	0.88 −2	0.37 −2	0.17 −2	0.96 −3
110	0.11 −1	0.94 −2	0.33 −2	0.15 −2	0.81 −3
120	0.12 −1	0.10 −1	0.31 −2	0.14 −2	0.75 −3
130	0.13 −1	0.11 −1	0.29 −2	0.13 −2	0.70 −3
140	0.14 −1	0.11 −1	0.28 −2	0.12 −2	0.64 −3
150	0.15 −1	0.11 −1	0.26 −2	0.11 −2	0.63 −3
160	0.16 −1	0.10 −1	0.24 −2	0.11 −2	0.63 −3
170	0.17 −1	0.94 −2	0.23 −2	0.11 −2	0.60 −3
180	0.17 −1	0.94 −2	0.23 −2	0.11 −2	0.51 −3

[a]The negative number in each entry is the exponent of 10 by which the cross-section on value should be multiplied.

which is probably as strong as that between these states and the $1\,^1S$ state, brings theory and experiment into much closer agreement. The same remarks also apply to Sec. IID which describes $2\,^3S$ excitation.

E. $1\,^1S$-$2\,^3S$ excitation of helium

Table X and Figs. 14–17 give results of the present five-state close-coupling calculation. In Fig. 14, for 29.6 eV, we compare the experimental cross sections obtained by Trajmar[32] and Hall *et al.*[33] with our theoretical cross sections and those of Thomas *et al.*[13] and Scott and McDowell.[12] A prominent dip at 125° was obtained by Thomas and Nesbet[37] in a preliminary calculation using a matrix variational method. They attributed their improved agreement with experiment compared to that of Thomas *et al.* to the coupling of $2\,^3S$ and $2\,^3P^0$ levels. In addition, in Fig. 15, for 40.1 eV, we compare with measurements of Yagashita *et*

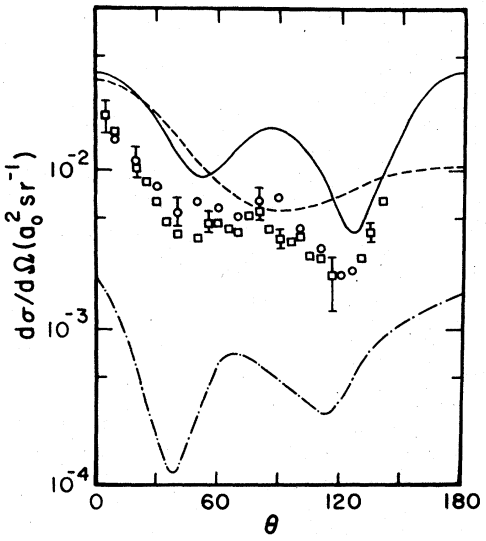

FIG. 14. Differential cross section for $1\,^1S$-$2\,^3S$ at incident electron energy of 29.6 eV. Symbols are given in Table V.

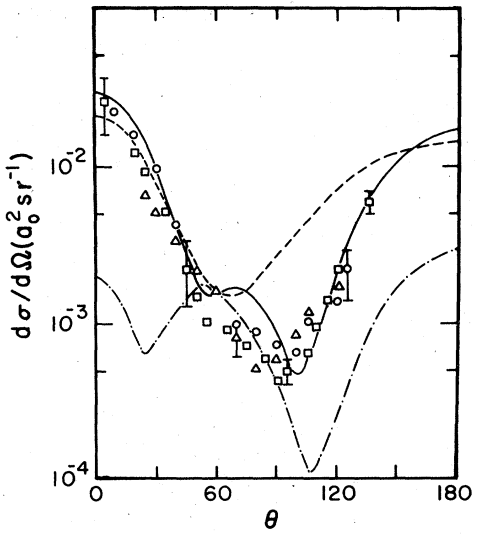

FIG. 15. Differential cross section for $1\,^1S$-$2\,^3S$ at incident electron energy of 40.1 eV. Symbols are given in Table V.

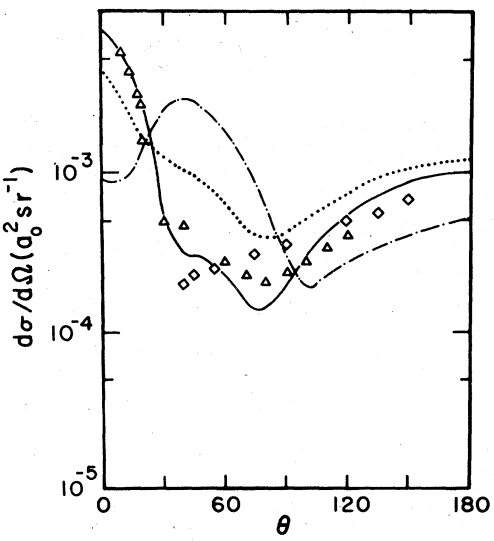

FIG. 16. Differential cross section for $1\,^1S$-$2\,^3S$ at incident electron energy of 80 eV. Symbols are given in Table V.

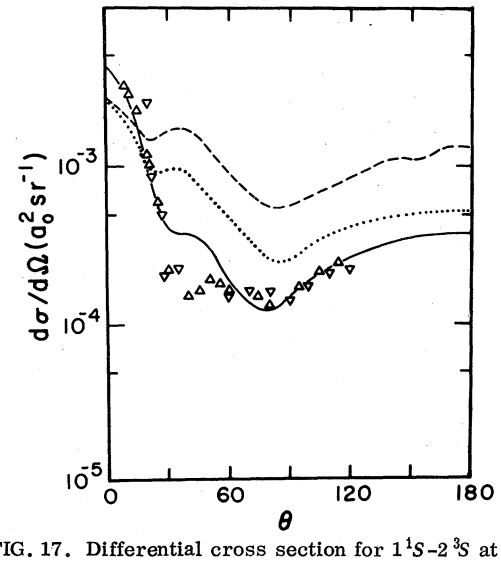

FIG. 17. Differential cross section for 1^1S-2^3S at incident electron energy of 100 eV. Symbols are given in Table V.

al.[36] Figure 16 compares present theory with that of Scott and McDowell[12] and Bransden and Winters,[10] and with the experimental results of Opal and Beaty[30] and Yagashita *et al.* for 80 eV. Finally, Fig. 16, for 100 eV, compares 5 CCX, MBT[13] and SOPDW[10] results with the measurements of Suzuki and Takayanagi[31] and Yagashita *et al.*

The main feature of the differential cross section for excitation of 2^3S is the existence of two minima at 50° and 125° for scattering of 29.6-eV electrons. The position of the second minimum moves inwards to 80° as the energy is increased to 100 eV, while the first minimum collapses to a shoulder. Present results show very good qualitative agreement with experiment, and for electron energies greater than 40 eV there is good quantitative agreement.

III. CONCLUSIONS

The present five-state close-coupling calculations are in very good qualitative agreement with measured shapes of differential excitation cross sections versus angle for energies in the range 29.6–100 eV. Neglect of higher states in the close-coupling expansion is expected to be the cause of the overestimation of the calculated excitation cross sections. In particular, differential cross sections at large scattering angles are too large when compared with experiment for excitation of 2^1S and 2^1P^0. Allowance for coupling between 2^3S and 2^3P^0 states in the present approximation brings calculated differential cross sections into good quantitative agreement with experiment for excitation to these states.

ACKNOWLEDGMENT

The research reported was supported in part by the U. S. Department of Energy under Contract No. EY-76-S-05-4881.

[1]B. H. Bransden and M. R. C. McDowell, Phys. Rep. 46, 249 (1978).
[2]D. G. Truhlar, J. K. Rice, A. Kuppermann, S. Trajmar, and D. C. Cartwright, Phys. Rev. A 1, 778 (1970); K. C. Mathur and M. R. H. Rudge, J. Phys. B 7, 1033 (1974).
[3]L. Vainstein, L. Presnyakov, and I. Sobelman, Zh. Eksp. Teor. Fiz. 45, 2015 (1963) [Sov. Phys. JETP 18, 1383 (1964)].
[4]F. T. Chan and S. T. Chen, Phys. Rev. A 8, 2191 (1973).
[5]M. R. Flannery and K. J. McCann, J. Phys. B 8, 1716 (1975).
[6]C. J. Joachain and R. Vanderpoorten, J. Phys. B 7, 817 (1974).
[7]K. A. Berrington, B. H. Bransden, and J. P. Coleman, J. Phys. B 6, 436 (1973).
[8]D. H. Madison and W. N. Shelton, Phys. Rev. A 7, 499 (1973).
[9]M. B. Hidalgo and S. Geltman, J. Phys. B 5, 617 (1972).
[10]B. H. Bransden and K. H. Winters, J. Phys. B 8, 1236 (1975).
[11]T. Scott and M. R. C. McDowell, J. Phys. B 8, 1951 (1975).
[12]T. Scott and M. R. C. McDowell, J. Phys. B 9, 2235 (1976).
[13]L. D. Thomas, G. Csanak, H. S. Taylor, and B. S. Yarlagadda, J. Phys. B 7, 1719 (1974).
[14]U. Fano, Comments At. Mol. Phys. 1, 159 (1970).
[15]P. G. Burke and T. G. Webb, J. Phys. B 3, L131 (1970).
[16]R. J. W. Henry and J. J. Matese, Phys. Rev. A 14, 1368 (1976).
[17]R. J. W. Henry, J. J. Matese, and W. L. Van Wyngaarden, Phys. Rev. A 17, 798 (1978).
[18]E. Clementi, J. Res. Dev. 9, 2 (1965).
[19]A. Hibbert, Comput. Phys. Commun. 9, 141 (1972).
[20]K. A. Berrington, P. G. Burke, and A. L. Sinfailam, J. Phys. B 9, 1459 (1975).
[21]C. E. Moore, U. S. Natl. Bur. Stand. Circ. No. 467 (1949) (unpublished).
[22]A. Weiss, J. Res. Natl. Bur. Stand. Sec. A 71, 163 (1967).
[23]E. R. Smith and R. J. W. Henry, Phys. Rev. A 7, 1585

(1973).
[24]K. A. Berrington, P. G. Burke, J. J. Chang, A. T. Chivers, W. D. Robb, and K. T. Taylor, Comput. Phys. Commun. 8, 149 (1974).
[25]M. A. Brandt, D. G. Truhlar, and R. L. Smith, Comput. Phys. Commun. 5, 456 (1973).
[26]R. H. J. Jansen, F. J. deHeer, H. J. Luyken, B. van Wingerden, and H. J. Blaauw, J. Phys. B 9, 185 (1976).
[27]M. V. Kurepa and L. Vuskovic, J. Phys. B 8, 2067 (1975).
[28]D. G. Truhlar, S. Trajmar, W. Williams, S. Ormonde, and B. Torres, Phys. Rev. A 8, 2475 (1973).
[29]A. Chutjian and S. K. Srivastava, J. Phys. B 8, 2360 (1975).
[30]C. B. Opal and E. C. Beaty, J. Phys. B 5, 627 (1972).
[31]H. Suzuki and T. Takayanagi, Abstr. VIII ICPEAC, 286 (1973).
[32]S. Trajmar, Phys. Rev. A 8, 191 (1973).
[33]R. J. Hall, G. Joyez, J. Mazeau, J. Reinhardt, and C. Schermann, J. Phys. (Paris) 34, 827 (1973).
[34]J. K. Rice, D. G. Truhlar, D. C. Cartwright, and S. Trajmar, Phys. Rev. A 5, 762 (1972).
[35]L. Vriens, J. A. Simpson, and S. R. Mielczarek, Phys. Rev. 165, 7 (1968).
[36]A. Yagashita, T. Takayanagi, and H. Suzuki, J. Phys. B 9, L53 (1976).
[37]L. D. Thomas and R. K. Nesbet, Abstr. IV ICAP, 468 (1974).